frontiers in Earth Science

ORIGINAL RESEARCH
published: 22 April 2020
doi: 10.3389/feart.2020.00103

The Anomalously Old Bush Stream Rock Avalanche and Its Implications for Landslide Inventories in Dynamic Landscapes

*Samuel T. McColl**

Geosciences Group, School of Agriculture and Environment, Massey University, Palmerston North, New Zealand

Previous dating of rock slope failures in most glaciated mountain chains has revealed almost exclusively young, mostly Holocene ages. In this study, a rock avalanche in the glaciated Rangitata Basin in Canterbury, New Zealand is mapped, described, and dated, revealing a pre-Holocene age of failure. The geomorphology and characteristics of the rock avalanche, named here as the Bush Stream Rock Avalanche, were assessed from field mapping and photogrammetric analyses. To assess the age of the rock avalanche, *in situ* cosmogenic ^{10}Be exposure dating was applied to boulders on the deposit. The geomorphological mapping shows that the morphology of the head scarp and deposit of the rock avalanche are distinct from the surrounding landscape, much of which appears to be glacial in origin. The rock avalanche traveled about 4 km, with a volume of 50–100 M m^3, and appears to have temporarily blocked Bush Stream. The dated boulders suggest an age of >16 ka (and likely >20 ka), making it the oldest reported alpine rock avalanche in New Zealand, and one of the oldest last-glaciation rock avalanches to be reported worldwide. Deep depressions, possibly kettle holes, in the deposit are indicative of runout over a glacier (or associated dead ice), but any glacier present at the time must have been small and probably decaying. The excellent preservation was likely favored by a small catchment located on the dry lee side of the Two Thumb Range which dampened glacial and fluvial activity. The study confirms that rock avalanches were being produced in the Southern Alps early in the last glaciation or early period of deglaciation, but that evidence for them likely exists only in the rare environments that have conditions favorable for preservation. Preservation potential in most of the Southern Alps is low, with older deposits readily buried or eroded by New Zealand's high rates of erosion, aggradation, and dynamic processes. Unless methods can be developed to identify missing older events, we are hampered in our ability to understand the frequency, and therefore causes, of large slope failures in the Southern Alps and in other highly dynamic alpine landscapes.

Keywords: mass movement, glacial geomorphology, cosmogenic surface exposure age dating, landform preservation, New Zealand, two thumb range

OPEN ACCESS

Edited by:
Tim Davies,
University of Canterbury, New Zealand

Reviewed by:
José DARROZES,
UMR 5563 Géosciences Environnement Toulouse (GET), France
Fabio Matano,
Italian National Research Council, Italy

***Correspondence:**
Samuel T. McColl
s.t.mccoll@massey.ac.nz

Specialty section:
This article was submitted to Quaternary Science, Geomorphology and Paleoenvironment, a section of the journal Frontiers in Earth Science

Received: *30 January 2020*
Accepted: *23 March 2020*
Published: *22 April 2020*

Citation:
McColl ST (2020) The Anomalously Old Bush Stream Rock Avalanche and Its Implications for Landslide Inventories in Dynamic Landscapes. Front. Earth Sci. 8:103. doi: 10.3389/feart.2020.00103

INTRODUCTION

In mountainous landscapes rock slope failures (RSFs) are a major hazard (Froude and Petley, 2018) and contributor to erosion and sediment generation (Korup et al., 2007; Korup, 2008). This is especially true in tectonically active mountains where high uplift rates and seismic activity generate abundant RSFs (Korup, 2005; Tatard et al., 2010; Görüm, 2019). This propensity may be further heightened in glaciated mountains where glacially steepened relief combined with glacier recession, periglacial activity, and glacial isostasy can trigger or further prime slopes for failure (McColl, 2012). The hazardous potential of RSFs and their apparent efficacy as a landscape process is largely inferred from examination of their modern-day topographic signatures, documented historical events, and often-incomplete inventories. Any attempts to reliably quantify or model their hazard or roles in landscape processes needs to be founded upon robust empirical data that captures representative information about their location, frequency, magnitude, characteristics, and their preparatory factors or triggers through time (i.e., over longer than historical timescales; Korup and Clague, 2009). This requires rich inventories of dated RSFs that can be compared against records of other landscape processes (e.g., climate, glacial activity, seismicity). However, in humid and tectonically active mountains, high sediment yield and dynamic landscape processes rapidly erode or mask RSF deposits and remove evidence. This can occur through burial by fluvial, glacial, or other mass movement sediments, reworking of deposits by glaciers or rivers, or obscuring by vegetation or water bodies (Cook et al., 2013; Dunning et al., 2015; Bainbridge, 2017; Schleier et al., 2017). This makes examining longer-term trends in RSF activity challenging, especially prior to the last deglaciation. Furthermore, while the frequency of RSF activity in the historical past tends to be better documented, pre-historical patterns of RSF activity, which may reflect major shifts in climate or other disturbance events (e.g., earthquakes), need the application of absolute dating methods (Pánek, 2019). Despite the recent upturn in the number of RSFs that have been dated worldwide, there are still few mountains in which the populations of known RSFs have been extensively and robustly dated (McColl, 2012; Pánek, 2014, 2019). In places where RSFs have been dated, new insights have emerged (see Pánek, 2019 for a review). For example, the age distributions of postglacial RSFs in the Scottish Highlands suggest the likelihood of a period of high-magnitude earthquakes induced by glacioisostasy (Ballantyne et al., 2014). To develop accurate RSF models and hazard forecasts, we need to recognize, reduce, and account for preservation bias, and expend effort in dating the RSFs we recognize in the landscape. As an incremental advance toward this goal, the aim of this present study is to describe and date a large rock avalanche deposit in the New Zealand Southern Alps. The RSF, named here as Bush Stream Rock Avalanche (BSRA), is mapped and its morphology and geometry analyzed from the field observations and aerial photography. The age of the event is assessed using cosmogenic nuclide exposure dating. The results suggest that, while its size and occurrence are not exceptional, its age, the depositional environment in which it was emplaced, and its preservation in the landscape are unusual for glaciated mountains.

STUDY SITE AND SETTING

The BSRA is situated within the Bush Stream catchment, a tributary of the Rangitata River, in the Canterbury High Country of New Zealand's Southern Alps (−43.72; 170.75; **Figure 1**). The ($\sim 2.5\ km^2$) rock avalanche deposit (∼1200–1500 m asl) occupies part of a small intermontane basin between the southern-central Two Thumb Range to the west and the smaller Sinclair Range to the east (**Figure 1C**). The rock avalanche fell from the northern slopes of a ridge connecting the two ranges (**Figure 1C**). The ranges are composed of Permian-Triassic Rakaia Terrane greywacke (sandstone and mudstone) (Cox and Barrell, 2007), with local peaks exceeding elevations of 2000 m above sea level. The block-faulted ranges are located some 55 km east of the plate boundary (Alpine Fault), on the Pacific Plate, and with the active Fox Peak and Forest Creek reverse faults within a few kilometers of the rock avalanche source area. Recurrence intervals for major earthquakes ($>M_w$ 7) on these faults may be 2000–3000 years (Stahl et al., 2016a,b). Stirling et al. (2012) estimate a regional probabilistic peak ground acceleration of 0.7–0.8 g over a 2500-year return time. Earthquake shaking is therefore a likely trigger for RSFs in this steep terrain.

The modern climate of the basin and surrounding hills is sub-alpine to alpine, with areas of rock and scree exposed on higher slopes, and tussock grasses and alpine vegetation in the lower basin. In the lee of the main topographic divide between the western and eastern alps and the Two Thumb Range, this area of the Southern Alps is relatively dry compared to other parts of the central alps which can reach 15 m of average annual rainfall (Kerr et al., 2011). The Bush Stream basin has an annual rainfall of ∼1.5 m (from 1972–2016), and median annual average temperatures of 7°C in the lower elevations to below 2°C on the higher peaks (from 1981–2010), estimated from 500 m grids of interpolated rainfall and temperature data (New Zealand Institute of Water and Atmospheric Science [NIWA]). There are no climate stations in the basin to validate these estimates, with the nearest being ∼13 km away. It is unknown what proportions of the precipitation falls as rain and snow, but some snow accumulation occurs in the winter months, as indicated by satellite imagery. Active periglacial processes (sub-zero temperature fluctuations) are likely to affect the higher slopes. Rock glaciers have been mapped in the Two Thumb ranges and some in the higher, northern parts of the range are likely still active where permafrost presence is modeled (Sattler, 2016; Sattler et al., 2016). No glaciers presently exist in the central Two Thumb range but there are cirque glaciers (mostly >1900 m asl) and a few small valley glaciers (terminating >1200 m asl) in the northern part of the range, 20–30 kilometers farther north.

Glacial activity was far more extensive during the Otira Glaciation (∼65–11.5 ka; Barrell, 2011) in the Two Thumb Range (Brook et al., 2006) and wider Rangitata Catchment with the limits of the Rangitata Glacier extending to the Rangitata Gorge

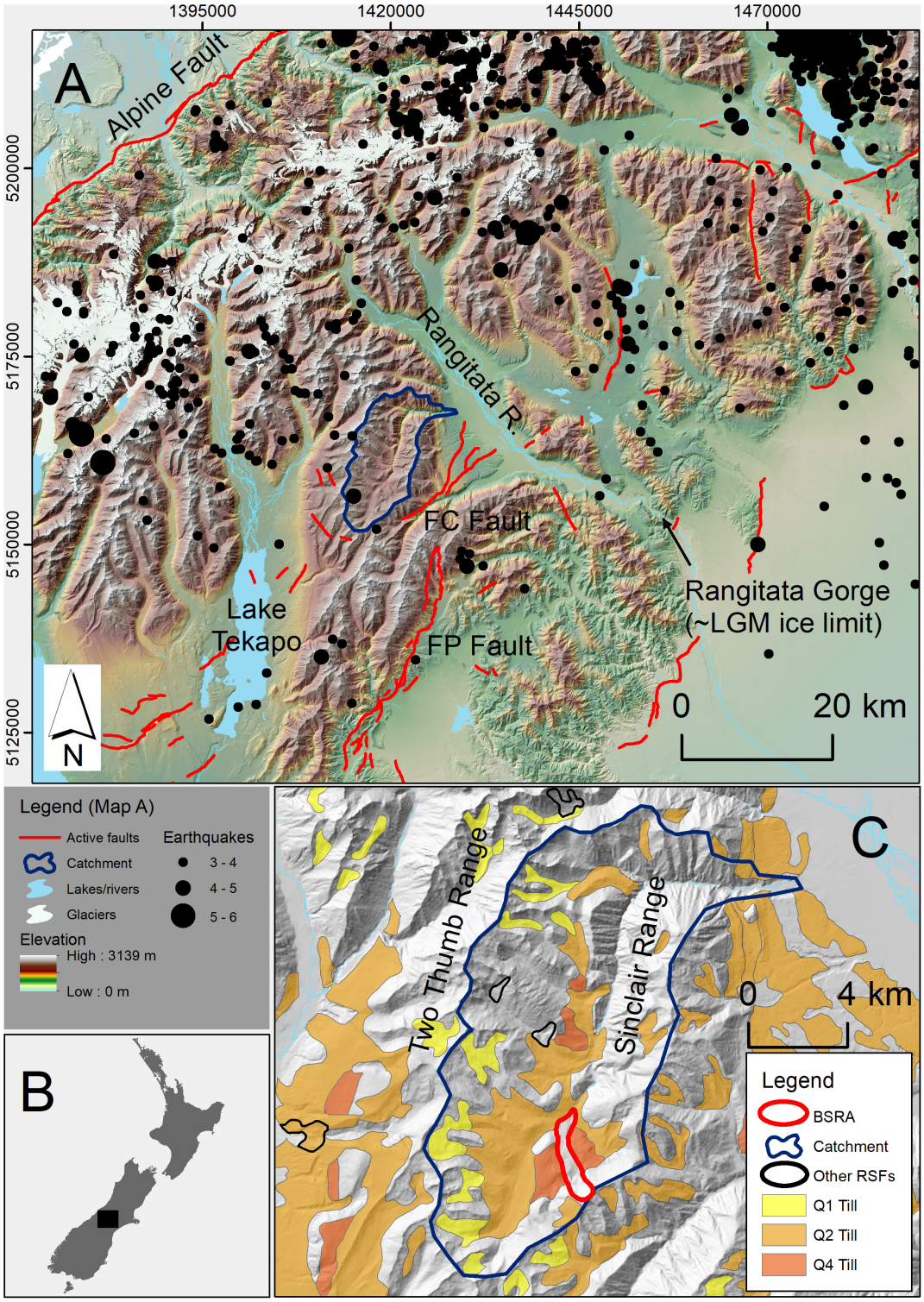

FIGURE 1 | (A) Location of Bush Stream catchment (blue outline), a tributary of the Rangitata River, within the eastern Southern Alps of New Zealand. Identified active faults are shown in red, sourced from the Institute of Geological and Nuclear Sciences (GNS Science) active faults database; http://data.gns.cri.nz/af/. The Alpine Fault, Forest Creek (FC) Fault, and Fox Peak (FP) Fault are labeled. The location of earthquakes (>M3) within the past 30 years (1990–2020) are shown from the GeoNet Earthquake Catalog, with indicated magnitude; the method of magnitude estimate varies in the catalog. The extant glaciers are shown in white. The approximate LGM extent of the Rangitata Glacier was at the Rangitata Gorge (labeled on map). The topographic data (colored hillshade model) are from LINZ: https://data.linz.govt.nz/. **(B)** Map of New Zealand with the location of Map A shown by the black rectangle. **(C)** Map showing the general topography of the Bush Stream catchment [same blue polygon as in Map **(A)**] with the Bush Stream Rock Avalanche (red polygon) and other landslides in the area (black polygons), along with the location of glacial sediments (till gravels) as mapped by Cox and Barrell (2007).

(<500 m asl) (Barrell, 2011; Shulmeister et al., 2018). Little is known of the extents of valley ice in Bush Stream basin, but evidence of glacial activity in the area is represented by cirque basins and till deposits (Cox and Barrell, 2007; Brook et al., 2008). Tills inferred to be of Late Pleistocene Age (Marine Isotope Stage [MIS] 2; 12–24 ka and MIS 4; 59–71 ka) are mapped in the Bush Stream basin while tills inferred to be of Late Pleistocene to Holocene Age (MIS 1–2; 1–14 ka) are mapped in the cirques above the Bush Stream basin (Cox and Barrell, 2007; **Figure 1C**). Like in many other parts of the Southern Alps (Kirkbride and Matthews, 1997; Brocklehurst and Whipple, 2007), the glacial activity in the Rangitata and tributary catchments has likely contributed to the generation of relief and steep rock slopes (Brook et al., 2008). Glacial steepening and growth of relief, along with deglaciation (e.g., glacial debuttressing, degradation of permafrost) are preparatory factors for rock slope failure (McColl, 2012). Consequently, rock slopes around Bush Stream may have experienced heightened instability conditions as a result of the Otira Glaciation and its transition toward Holocene conditions. Several RSFs and rock avalanches have been mapped in the Two Thumb ranges, but the BSRA appears to be the largest of these. The BSRA had first been mapped by Cox and Barrell (2007), who inferred it to be of Holocene age. It fell from a north-west facing slope in the southern part of the Bush Stream catchment (**Figure 1C**), likely from glacially modified slopes.

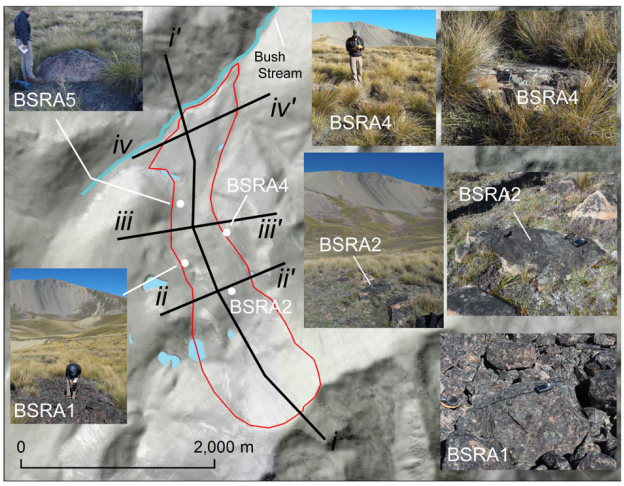

FIGURE 2 | Approximate extent of the Bush Stream Rock Avalanche (red outline; see **Figure 1C**) with locations of the long-section (black line i) spanning the length of the rock avalanche and cross-sections of the deposit (black lines; proximal ii; central iii; and distal iv), and ^{10}Be sample locations (white dots labeled BSRA#) with corresponding photos showing sampled boulder or surrounding ground. Lakes are indicated in blue. The base image of the main map is a semi-transparent LINZ 8 m hillshaded DEM overlaid onto LINZ aerial imagery.

MATERIALS AND METHODS

Topographic Data

The best existing topographic data for the area was the Land Information New Zealand (LINZ) national 8 m digital elevation model (DEM) which is based on interpolation of photogrammetrically derived 20 m contours. To provide a higher resolution topographic data set for mapping the rock avalanche deposit extent, visualization of the deposit morphology, and terrain analysis, a new topographic dataset was produced using Structure from Motion (SfM) photogrammetry. A photogrammetry survey was undertaken in March 2016 using a Phantom three Professional remotely piloted aircraft, capturing ∼1250 photos from 100–120 m above ground level, and mostly overlapping at better than 60% side and 70% forward overlap with a combination of nadir and oblique images. Seventeen ground control points (1 m canvas squares) were distributed on and around the rock avalanche deposit, and surveyed with a Trimble R10 GNSS receiver that was differentially corrected against the Mount John Observatory (MTJO) continuous GNSS station (at a 37 km baseline distance). The 2016 New Zealand Geoid Model was used to convert ellipsoidal elevations to orthometric heights, providing all survey data heights relative to the 2016 New Zealand Vertical Datum (NZVD2016), which approximates sea level. Differential correction resulted in point precisions of better than 0.08 m (horizontal and vertical) with an accuracy estimated to be better than 0.1 m (H&V) after accounting for error in GPS receiver pole placement on the ground control centroid. SfM photogrammetry processing was done with Agisoft Metashape 1.5.2. The initial alignment was done using the highest accuracy settings, the sparse cloud was edited to remove tie points of high uncertainty and georeferencing was applied prior to camera optimization and dense cloud generation. The ground control point RMS error was 0.43 m with a min. and max. error of 0.09 and 1.10 m, respectively. A 0.5 m digital surface model (DSM) was produced along with an orthophoto mosaic. No independent topography data were collected in the field to assess the accuracy of the SfM model, so forty manually selected check points were used to evaluate the consistency between the SfM-derived DSM and the national 8 m DEM (which has a stated accuracy of 90% of well-defined points falling within ±10 meters vertically). The min, RMS and max vertical differences of the forty check-points were 0.1, 7.7, and 14.0 m, respectively, with 95% of points having a difference of less than 8.2 m, consistent with the uncertainties estimated for the 8 m DEM. The SfM data were therefore deemed to be of sufficient accuracy for use in the geomorphological mapping and coarse-scale terrain analyses of this study.

Geomorphological Mapping and Rock Avalanche Geometry

The outline of the rock avalanche deposit, major topographic features (scarps or depressions), and hydrological features (streams or drainage lines) were mapped using a hillshade model derived from the 0.5 m DSM, an orthophoto mosaic (from the SfM), and from field observations. The complete source area of the rock avalanche was not captured in the photogrammetric survey (SfM DSM), so the 8 m LINZ DEM was used for mapping and terrain analysis of the rock avalanche source area. The planimetric areas for both source area and the deposit were measured. A long-section from the top of the source area to the

inferred most-distal extent of the rock avalanche was drawn and the pre-existing travel path was roughly interpolated (Section *i* in **Figure 2**). The travel angle (fahrböschung) was calculated [$\tan^{-1}$ (fall height/runout length)] and compared against travel angles for other rock avalanches of a similar size. Cross-sections were extracted for proximal, central, and distal parts of the deposit to help support the mapping of the deposit extent and estimates of deposit thickness for volume calculations. Deposit thickness was roughly estimated from the cross-sections, by manually interpolating the pre-existing topography (valley floor) between the deposit margins. This interpolation is less confident in the central and proximal parts of the deposit, but is more confident at the distal end where the pre-existing river terraces are visible and suggest a relatively planar surface may have existed. To account for the uncertainty in the position of the pre-existing ground surface, and subsequent loss of rock avalanche material from erosion, an upper and lower bound estimate of deposit thickness was adopted.

To estimate the volume of the rock avalanche three methods were used: (i) The cross-sections (**Figure 2**) were used to estimate an average (upper and lower bound) deposit thickness which was then multiplied by the mapped deposit area; (ii) An area-volume scaling relationship for rock avalanches (Figure 1 in Hungr, 2006) was used to estimate the likely volume of the rock avalanche from the mapped area of the deposit; (iii) The source scar volume was estimated by reconstructing the pre-failure topography of the source scar, assuming that the hillslope that failed was an approximately planar slope, similar to the adjacent north-eastern slope. An 8-m DEM was produced to represent this pre-failure topography and differenced against the present-day 8-m DEM to derive a volume for the scar. The volume of material removed from the scar will have undergone bulking from fragmentation, a process which can increase rock avalanche volumes by some 15–25% (Jiskoot, 2011). Therefore, the source volume was increased by 20% to provide a deposit-volume equivalent. Additional bulking from entrainment during transport was not considered but may have further increased the volume of the deposit. The scar volume analysis also ignores post-failure erosion (i.e., enlarging) of the scar or materials accumulated in the scar (i.e., reducing scar volume estimate), and in general likely provides a lower-bound estimate of volume vacated from the scar. While all three methods suffer from different uncertainties and assumptions, it is considered that the three methods provide a realistic range for the volume of the rock avalanche.

Cosmogenic Dating

To assess the age of rock avalanche deposit, *in situ* cosmogenic ^{10}Be exposure dating was applied to three boulders exposed on the surface of the rock avalanche (**Figure 2**). One further sample (BSRA4; **Figure 2**) was taken from a boulder originally considered to be part of the rock avalanche, but later thought to be part of an adjacent slope failure. Soil development and weathering appears to have obscured or disintegrated many of the boulders so there were few suitable boulders to choose from for sample selection. However, to reduce the chance of selecting boulders or boulder surfaces that would provide unrepresentative exposure ages, the following sampling criteria were followed: (i) the boulders were larger than 1 m in diameter; (ii) the boulders were on gently sloping or flat ground and therefore less likely to have rolled/toppled since their original emplacement; and (iii) the sampled surface of the boulder was more than 0.2 m above any surrounding soil; (iv) the sampled surface was weathered (i.e., not recently exposed or over-turned). All samples appeared to be of similar lithology – slightly to moderately weathered, orange-gray greywacke sandstone. An angle-grinder, hammer and chisel were used to chip off approximately 1.5–4 cm thick layers of rock from the boulder surfaces, targeting quartz veins where available. Skyline horizon surveys were made at each sampled boulder location with a inclinometer and compass, for use in correcting for the topographic shielding of cosmogenic radiation. Boulder position was measured with a Garmin hand held GPS, but boulder elevation was measured from the SfM DSM.

Quartz was isolated from the greywacke samples following standard mineral separation procedures, following crushing, sieving, and acid washing. Beryllium targets were prepared at GNS Science and Victoria University of Wellington, in New Zealand. The beryllium of samples and two process blanks was measured by the GNS Science Accelerator Mass Spectrometer. Two processing blanks (KV322 and KV332) were averaged and the correction was less than 1.6% ($1.8 \pm 0.3 \times 10^5$ a ^{10}Be). Exposure ages, using processing-blank corrected data, were calculated using the online exposure age calculator (version 3; Balco et al., 2008). Corrections for sample thickness and topographic shielding were applied, with the shielding factor assessed using the online topographic shielding calculator. Sample densities were assumed to be 2.7 g/cm^3, a typical value for New Zealand greywacke (Hatherton and Leopard, 1964). The Putnam et al. (2010) Boundary Stream Tarn Moraine, New Zealand ^{10}Be production-rate calibration was used along with the time-dependent "LSDn" scaling scheme used to scale for elevation and latitude. ^{10}Be ages presented in this study are not corrected for erosion or snow shielding, both of which might have reduced ^{10}Be production leading to apparently younger ages. However, while no data are available on erosion rates on greywacke or time-dependent variations in snow-cover for Bush Stream catchment, an estimate of their potential effect was assessed. For erosion, erosion rates of 0.5 cm/ka and 1 cm/ka were applied in the online exposure age calculator. To evaluate snow shielding, the surface cover correction tool of Jones et al. (2019) was used with a snow density of 0.27 g cm^{-3} and a snow depth of 25 and 50 cm (representing a time-averaged snow depth for the entire exposure history). Note, these values are not constrained by any data but are considered to be upper (conservative) estimates for erosion and snow cover.

RESULTS

Rock Avalanche Characteristics

The rock avalanche deposit covers an area of 2.2 M m^2 and traveled ∼4 km from the top of the concave source area (∼2003 m asl) to the distal most extent of the mappable deposit (∼1180 m asl), representing a fall height of about 820 metres

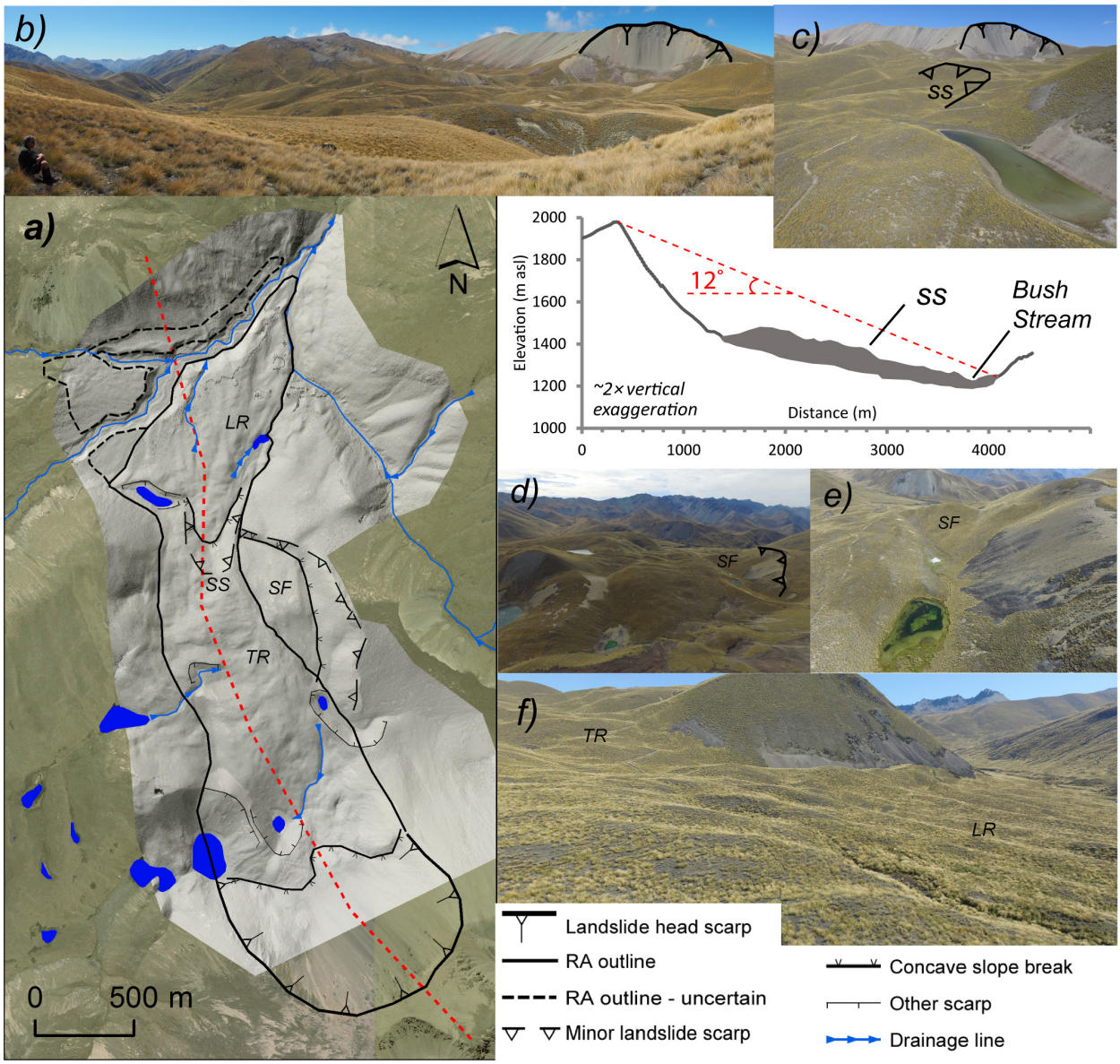

FIGURE 3 | (a) Geomorphological map of the Bush Stream Rock avalanche with corresponding long-section (dashed red line on map) with runout angle and inferred deposit shown in gray shading. Lakes are shown as blue on the map. The base image is the hillshaded 0.5 m SfM DEM on top of LINZ aerial imagery. LR = longitudinal ridges; SS = secondary scarp; SF = other slope failure; TR = transverse ridges. Supporting photos are provided to show some morphological features: **(b)** Photo taken from slope opposite distal end of deposit looking south toward the head scarp. **(c)** Photo looking southeast with view of the secondary scarp (SS) within the deposit. **(d)** Photo looking north-west along the rock avalanche deposit, taken from near the base of the head scarp, with several of the lakes visible, and the other slope failure (SF) abutting Bush Stream Rock Avalanche; **(e)** View looking north, with closer view of the other slope failure (SF); **(f)** View looking south-west from near the distal end of the deposit, showing narrow ridges (LR) aligned parallel to flow in the distal part of the deposit and shorter ridges (TR) aligned more transverse to flow in the mid reaches of the deposit.

and a travel angle (fahrböschung) of 12 degrees (**Figure 3**). The lateral margins of the deposit are mostly clearly distinguishable from the valley sides, especially on the eastern margin, expressed by a prominent edge that sharply contrasts with the pre-existing topography. The distal end of the deposit extends to the far side of Bush Stream, and appears to have super-elevated by some meters on the slopes at the northern side of Bush Stream, but its boundary is difficult to define. The rock avalanche likely blocked Bush Stream, and the stream has since cut through the deposit by 20–30 meters, providing one of the few exposures of the internal fabric of the deposit (**Figure 4**), which shows a poorly sorted, very angular to sub-angular diamicton with boulders through to fine particles. Rounded boulders and cobbles are visible in places at the base of the stream exposure, of similar nature to the modern boulders in Bush Stream. In most other locations little of the rock avalanche material is visible beneath the tussock grasses, with

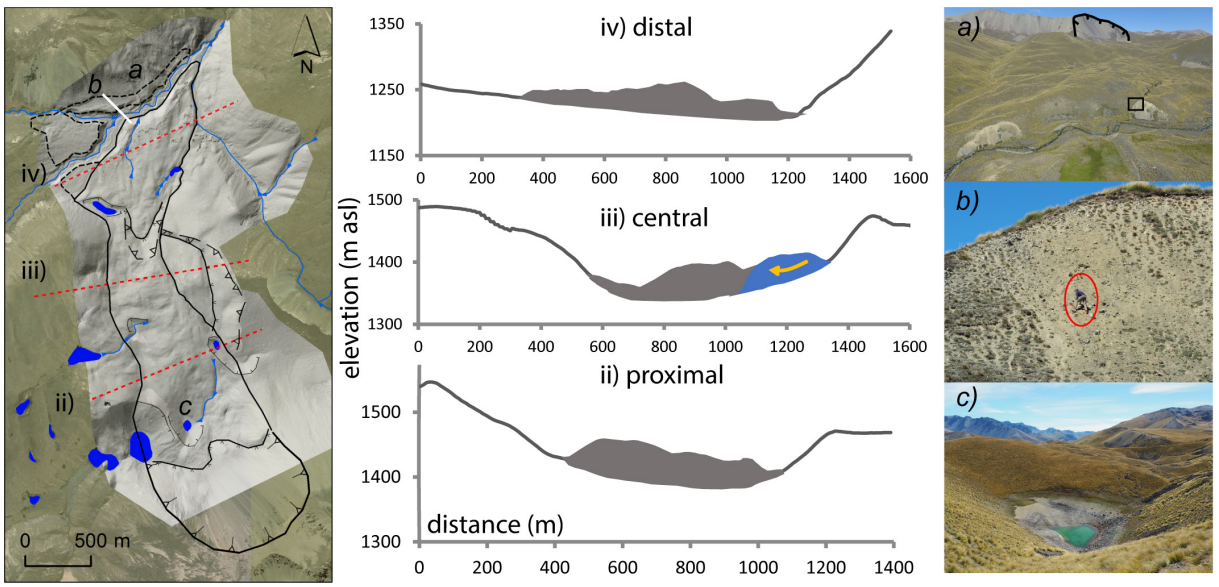

FIGURE 4 | Cross-sections ii-iv of rock avalanche deposit with locations of the sections and field photos indicated on map on the left. Photo **(a)** looking southwards with a view of Bush Stream in the middle distance and the source area crown (marked as black scarp) on the horizon. **(b)** Exposed rock avalanche sediments along Bush Stream (approx. photo position shown with black rectangle in photo **(a)**, showing the lack of stratification and poor sorting of deposit. **(c)** One of the depressions with a small lake within the rock avalanche deposit, with location indicated on the map on left.

shattered gravel- to small boulder-sized clasts visible in patches, but few large boulders, and no open-framework, large-boulder carapace typical of some rock avalanche deposits.

The body of the rock avalanche is undulating-hummocky with broad (30–100 m wide) but uneven ridges, which in the proximal and central deposit tend to be transverse to flow, and in the distal deposit are longitudinal to flow, narrower, and more elongate (**Figure 3**). The deposit appears (based solely on cross-section interpolation) to be approximately 20–70 meters thick in the upper to mid sections of the deposit, thinning to 20–30 m thick in the more distal section (**Figure 4**). A 10–50 m high arcuate-triangular secondary scarp (SS in **Figure 3**) separates the distal and mid-upper sections of the deposit, suggesting a secondary surge in the flow (see Strom, 2010), presumably as it dropped onto the Bush Stream floodplain and spread out due to a reduction in confinement. The lateral spreading may also explain the transition in this location to longitudinal ridges (see Dufresne and Davies, 2009). In several locations on the rock avalanche deposit there are (∼10–60 m) deep depressions, most of which host small lakes. The largest of these is in the south-western margin of the rock avalanche deposit (i.e., near the source area), but smaller depressions occur in the distal part of the deposit (**Figure 3**). These isolated depressions tend to deviate from the more subtle undulating-hummocky topography of the deposit.

The volume of the deposit calculated from the cross-section interpolation ranges between 71 and 107 M m^3. Using the area to volume scaling relationship (Figure 1 of Hungr, 2006) suggests a volume of ∼70 M m^3 using an area of 2.2 M m^2. The volume calculated for the source scar is smaller than both of these estimates. The reconstructed scar thickness is up to ∼120 m with an average of 44 m and planimetric area of 0.995 M m^2. That gives a volume of 43.8 M m^3, or 52.4 M m^3 after accounting for 20% bulking from fragmentation. Taken together, the volume of the original rock avalanche deposit is likely to have been between 50–100 M m^3. Both the (12°) travel angle and (4 km) runout length are within the expected range for rock avalanche volumes over this range (Hungr, 2006).

Another, smaller slope failure appears east of the rock avalanche deposit, defined by an approximately 1-km long and 30–120 m high arcuate head scarp above a displaced block (SF in **Figure 3**). The arcuate nature of the scarp and otherwise intact block of material suggests failure as a rotational debris slide or rotational rock slide – no suitable exposures allowed the nature of the materials at depth to be examined. The slope failure appears to be onlapped at the toe by the rock avalanche debris (**Figure 4**) with no obvious deformation of the rock avalanche deposit in this location, indicating that its movement/emplacement preceded (even if narrowly) the rock avalanche.

Cosmogenic Dating

The three boulders on the rock avalanche deposit have ^{10}Be exposure ages and external errors of 15.2 ± 0.5, 19.8 ± 0.5, and 20.1 ± 0.5 ka, and the boulder on the smaller slope failure east of the rock avalanche deposit has an exposure age of 16.6 ± 0.5 ka (**Table 1**). These ages do not account for erosion or shielding by snow cover. Applying erosion rates of 0.5 and 1 cm/ka, increases the ages by 1.1–1.8 ka (∼6-8%) and 2.4–4.3 ka (∼15–21%) respectively. Incorporating 25 and 50 cm of time-averaged snow-cover increases the ages by 0.7–0.9 (4–5%) and 1.4–1.8 ka (9–10%) respectively. The ages could therefore be some 10–30% older.

TABLE 1 | Cosmogenic ^{10}Be exposure age parameters and results. All samples were considered to have a density of 2.7 g cm^{-1}, a typical value for greywacke, and measured with the same AMS standard, 07KNSTD.

Sample name	Latitude	Longitude	Elevation (m asl)	Thickness (cm)	Shielding correction	Be-10 ± 1 σ (atoms g^{-1})	Age ± 1 σ (years) (external error in brackets)
BSRA1	−43.722	170.754	1429	2.5	0.998	197,013 ± 5,433	15,213 ± 421 (460)
BSRA2	−43.720	170.759	1434	2.0	0.996	265,082 ± 5,174	20,118 ± 395 (465)
BSRA4	−43.719	170.759	1408	3.5	0.997	210,106 ± 5,468	16,611 ± 434 (479)
BSRA5	−43.716	170.753	1343	1.5	0.994	241,861 ± 4,871	19,821 ± 401 (468)

To explain the ∼5 ka difference in exposure age between the youngest and the two older samples on the rock avalanche deposit, either the older samples both incorporate inherited ^{10}Be and/or the younger sample has a burial or erosion history that results in a lower ^{10}Be concentration. Hilger et al. (2019) have suggested that rock avalanches are prone to surface boulders with ^{10}Be inherited from previous exposure. This is due to rock avalanche materials typically not being vertically mixed during transport, resulting in a high chance of surface boulders being sourced from at or close to the original ground surface of the failed rock slope. This inheritance effect is smaller for older (>Holocene) RSFs on the assumption that glaciation or other processes sufficiently eroded, and therefore, reset the exposure history of the rock slope (Hilger et al., 2019). There is insufficient information to constrain ice thickness in the Bush Stream basin but likely parts of the rock slope were glacially eroded in the last glaciation given the evidence of glacial deposits (tills) mapped in the valley. Further, even if not significantly glacially eroded, the rockslope surface is likely to have undergone erosion by frost-weathering and rockfall processes, given its elevation (1600–2000 m asl) and steep gradient (>30 degrees; as measured for the adjacent unfailed hillslope). These erosion processes would have limited the amount of inherited ^{10}Be likely to be found in the rock avalanche samples.

Another explanation for the age difference is that the younger sample on the rock avalanche (BSRA1; 15.2 ± 0.5 ka) may have experienced ^{10}Be loss through erosion. The sample was taken from a boulder field in which boulders there were noted to be undergoing exfoliation/flaking, probably driven by frost weathering. Evidence of exfoliation was not noted for the other two rock avalanche samples, and therefore sample BSRA1 may have experienced higher erosion (i.e., removal of ^{10}Be). Differences in the prevalence of exfoliation may relate to differences in fracturing induced in the boulders by the rock avalanche process, or slight (unrecorded) lithological variations in the greywacke. The boulder may have also experienced slightly greater snow cover than the other rock avalanche samples (especially BSRA5), as it is relatively more low-lying. These factors together may explain the ∼5 ka difference in age.

The boulder (BSRA4) on the smaller slope failure east of the rock avalanche deposit has an exposure age of 16.6 ± 0.5 ka. If the interpretation of a rotational slide is correct for this slope failure, then the boulders on its surface are unlikely to have been disturbed during movement. In this case the sample age represents the age of the glacial sediment rather than the slope failure. The contact between the rotational slope failure and the rock avalanche indicates that the slope failure predates the rock avalanche. The age of 16.6 ± 0.5 ka therefore either suggests, like with BSRA1, there may have been erosion of the boulder (again supported by the observation of exfoliation flakes for this boulder), or it represents the timing of glacier retreat from this hillslope, and the rock avalanche is younger than ∼16.6 ka. If the latter, then it would lend more support to the two older (∼20 ka) samples from the rock avalanche having inherited ^{10}Be and a younger (e.g., 15 ka) age being more likely for the BSRA. However, like with BSRA1, it is entirely feasible that heightened erosion (from exfoliation weathering), and snow cover, could have resulted in an exposure age younger than the older samples from the rock avalanche.

DISCUSSION

Implications for Rock Avalanche Inventories

Whether the younger ^{10}Be age or the two older ^{10}Be exposure ages are more representative of the age of the rock avalanche, the rock avalanche is an anomalously old rock avalanche for the Southern Alps and many other glaciated mountains globally (McColl, 2012), especially if the effects of erosion and snow cover are included (i.e., they are 10–30% older). Green Lake Landslide in Fiordland (∼350 km to the south-west), may be the only other rock slope failure/avalanche in the Southern Alps that is known to (perhaps) have a pre-Holocene age (of 12–13 ka; Hancox and Perrin, 2009). Its preservation is likely partly owed to the very sizeable nature of the deposit – having a volume of 27 km^3. All other pre-historic dated, disrupted RSFs and rock avalanche deposits in the New Zealand Southern Alps are of Holocene age (Bainbridge, 2017), with only four of those occurring in the Early Holocene (Whitehouse and Griffiths, 1983; Lee et al., 2009), and 13 within the Mid-Holocene (Whitehouse and Griffiths, 1983; Hancox et al., 2013; Sweeney et al., 2013; McColl et al., 2019). Another 50 or so are dated from the Late-Holocene with increasing apparent frequency, and more than 100 historically recorded events have occurred since the 1800s (Bainbridge, 2017). Whitehouse and Griffiths (1983) and Bainbridge (2017) recognize that the apparent increase in frequency of events in New Zealand is not a real increase in frequency. Rather, it reflects a strong censoring of mass movement deposits from the humid and tectonically active Southern Alps as a result of the rapid erosion, modification, burial, or masking of deposits by glaciers, rivers, sediments and vegetation. Further to that, while several hundred deposits are mapped, absolute-age information exists for only 66% or so and most of those are historical events within

the past 100 years (Bainbridge, 2017). The BSRA is therefore extremely old in the context of other dated mass movements in the Southern Alps, confirming that older events do exist but are likely to be no longer visible or simply not dated yet. The rapid censoring of deposits in New Zealand make it difficult to assess the true frequency of such events, and therefore make it difficult to reliably examine environmental processes driving changes in RSF activity. In contrast, in tectonically inactive mountains, such as the Scottish Highlands, post-glacial rock slope failure rates have been shown to be nearly five times higher prior to the Holocene, likely associated with enhanced seismicity (Ballantyne et al., 2014).

As more of the mapped deposits in the Southern Alps are dated, through greater application of absolute-age dating methods, there is potential to remove some of the age-bias and gaps in the frequency data. However, the development of other means of identifying and dating buried or reworked rock slope failure sediments may be necessary to reduce this bias sufficiently in order to draw meaningful evaluations of RSF frequencies. This will be necessary for supporting robust hazard assessments and for reliable assessment of the long-term bio-geomorphic impacts of rock avalanches or establishing of relationships between RSF frequency with that of climate changes or triggers such as earthquakes.

Insight Into the Depositional Environment and Climate of the Bush Stream Basin

The pre-Holocene timing of the rock avalanche means it occurred at a time when there was likely to still be a considerable volume of glacial ice in the Southern Alps and in the Rangitata Basin. While the local Last Glacial Maximum (LGM) in the Rangitata Catchment at c. 28 ka was earlier than the global LGM, the termination of the last glaciation was gradual from about 19–16 ka (Rother et al., 2014). Rother et al. (2014) suggest that substantial valley glaciers are likely to have been present in much of the Rangitata catchment until at least 15.8 ka. Mapping by Cox and Barrell (2007), albeit based on relative age assessment/geomorphic correlations, suggests that the rock avalanche fell onto tills of MIS 4 (∼59–71 ka) age, but that the distal end of the avalanche may have been emplaced onto tills of late glacial to Late Otira (MIS 2; 12–24 ka) age (**Figure 1C**). The data presented here suggests that the tills mapped near the distal end of the rock avalanche are at least older than 15–20 ka (i.e., older than the overlaying rock avalanche). The tills mapped as MIS 4 on the other hand may be younger (more likely MIS 2) than suggested by Cox and Barrell (2007). The boulder dated on the rotational slope failure east of the rock avalanche (BSRA4) has an age of at least 16 ka (likely several ka older after accounting for erosion and snow cover), and is most likely glacial sediment (as mapped by Cox and Barrell, 2007). The rotational movement of the slope failure does not appear to have caused disruption or deformation of the glacial materials, and even if the boulder was overturned during the slope failure (resulting in a younger exposure age), it is unlikely to be as old as MIS 4. This is supported by the observation of large depressions in the rock avalanche body. The depressions in the rock avalanche are much larger than the typical hummocky topography found on rock avalanches and which tend to show the inverse (i.e., large mounds rather than large holes). The depressions may be explained by the rock avalanche falling onto dead ice or an active glacier, either running over the glacier, or entraining blocks of the glacier, and the subsequent melt of the disintegrated ice blocks that produced "kettle holes". The largest kettle hole is on the western edge of the deposit, proximal to the source area where the rock avalanche deposit is inferred to be thickest. The depth of the lake occupying the bottom of this kettle hole is unknown but its surface is about 60 meters below the higher parts of the adjacent deposit, suggesting an ice thickness of some 60 m. If there was glacial ice (or at least "dead" ice) still present in the Bush Stream catchment at the time of the rock avalanche (c. 15–20 ka), it suggests that the glacial sediments mapped in this area are more likely of MIS 2 age.

An alternative explanation for the presence of the depressions in the deposit is that the depressions existed in the valley floor prior to the rock avalanche, possibly from older kettle holes produced by meltout of a sediment-covered glacier. However, a rock avalanche is likely to deposit sediment into any lake/depression it travels through, filling in those depressions. Therefore, it seems unlikely that these depressions existed, especially those below the rock avalanche source area where the deposit is thicker, prior to the rock avalanche. Although based on little data, taken together, the observation of the large depressions (kettle holes) and the age of the boulder on the rotational slide, provide some evidence that there was still glacier (dead?) ice present at the time of the rock avalanche, and that it was likely Late Otiran (MIS 2) in age.

If glacier ice is associated with the origin of the depressions, the remarkably good preservation of the rock avalanche deposit suggests that any glacier that the avalanche may have fallen onto was incapable of transporting or substantially modifying the RSF deposit, and it did not subsequently re-advance as far as the avalanche [e.g., during the Antarctic Cold Reversal (c. 14.7–13 ka), in which other glaciers in New Zealand advanced; Shulmeister et al., 2019]. When RSFs fall onto glaciers, they can increase the mass balance and induce an advance independent of climate, and the glaciers themselves are likely to modify RSF deposits, reworking the supraglacial sediment into moraines or entraining and modifying the sediment through active glacial transport processes (Shulmeister et al., 2009; Deline et al., 2015; Dunning et al., 2015; Reznichenko et al., 2015). There is no such morphological or sedimentological evidence to suggest that any of these processes (climate or mass movement-driven advance, or modification by glacial activity other than by dead-ice melt) occurred to any noticeable extent. These observations suggest the Bush Stream basin in the location of the rock avalanche at that time (15–20 ka) was either ice-free or had a glacier with a severely negative mass balance that was retreating, and that the rock avalanche did not sufficiently positively influence the glacier's mass balance.

These observations and the unusually good preservation of this deposit (for the Southern Alps), likely reflects the physiography of the Bush Stream basin. The catchment area

of the basin above the rock avalanche is small (<45 km^2), and although with topography above the tree line, it has lower elevations than the northern part of the Two Thumb Range, and therefore likely had a relatively small accumulation area for snow. The position of the catchment in the lee side of the Two Thumb Range, in a low-precipitation region of the Southern Alps further would have resulted in perhaps lower-than-average snow accumulation. These factors combined probably limited the mass balance, length and flow rates of any valley glacier in the catchment such that by 15–20 ka when the BSRA fell, it was either retreated beyond that location or sufficiently small to cause no substantial modification. Likewise, while Bush Stream was able to breach and erode some of the distal end of the deposit that had temporarily dammed it, neither it nor other tributary streams have been sufficient to substantially remove or bury the deposit. This again, likely reflects the dry climate, small catchment, and consequent low competency of the streams.

The Causes of the Bush Stream Rock Avalanche

While the exact factors that caused the BSRA remain unknown, it is reasonable to speculate that the event was triggered by strong earthquake shaking. The bowl morphology of the source area that extends to the top of the ridge is typical of co-seismic RSFs (McSaveney et al., 2000). Further, there are no apparent structural features in the source scar that suggest obvious structural weakening (e.g., exposed dip-slope bedding planes, major persistent joints or faults). There is no evidence of secondary scarps or antiscarps above or adjacent to the source scars, which might indicate some pre-failure deformation and a progressive failure mechanism that could bring the slope to failure in the absence of a significant trigger. The Forrest Creek and Fox Peak faults are both within 10 km of the source area and paleo seismic evidence and modeling by Stahl et al. (2016b) suggests they are capable of generating earthquakes much stronger than the M_w 6 threshold for co-seismic triggering of major RSFs in New Zealand (Hancox et al., 2002). Paleo seismic records for the faults do not extend as far back in time as the BSRA, but given the recurrence intervals for the faults of less than 3000 years (Stahl et al., 2016b), they are likely to have generated multiple earthquakes over the past 20,000 years.

By the end of the last glaciation, the slope may have been primed for failure in an earthquake from steepening of the slope by glacier erosion and subsequent changes during the initial stages of deglaciation. The melting and complete or partial retreat of any glacier may have removed slope support (i.e., glacial debuttressing), exposed the rock slope to a new thermal regime with enhanced frost weathering, and possibly enhanced the intensity of any co-seismic shaking by increasing the topographic amplification of seismic waves (McColl et al., 2012). If the latter (i.e., paraglacial processes were operating and had contributed to slope priming) it provides a relatively rare example of an early (in the deglaciation history) rockslope response to glacier retreat (c.f. McColl, 2012; Hermanns et al., 2017), similar to only a small number of (>15 ka) RSFs in the Scottish Highlands where the timing of post-glacial RSFs is well-recorded (Ballantyne et al., 2014) and few other examples globally (Pánek, 2019).

CONCLUSION

The BSRA is the oldest known rock avalanche in the Southern Alps of New Zealand, occurring earlier than ∼16 ka (likely >20 ka). A volume of 50–100 M m^3 fell from the steep greywacke bedrock hillslope, producing a concave depression in the rock slope, and transitioned into a rock avalanche which traveled 4 km and temporarily blocked Bush Stream. Eventually the river breached the dam, as indicated by a deep channel through the distal end of the deposit. A travel angle of 12 degrees and runout distance of 4 km for the rock avalanche is typical for an event of this volume. The undulating, ridge-like morphology of the avalanche is also fairly typical of rock avalanches, except for the presence of several large lake-filled depressions. These depressions are interpreted to have formed from the melt out of glacier ice (dead ice) that the rock avalanche overrode and possibly entrained. Other than these depressions and fluvial erosion by Bush Stream, the avalanche is remarkably well preserved for its age, especially given the tendency for the Southern Alps to rapidly erase or obscure evidence of mass movements. Preservation of such a deposit suggests small, receded glaciers in the early stages of the regional deglaciation, and incompetent rivers with low sediment load and discharge. These factors likely reflect the relatively small size and very dry climate of the catchment in the lee of a mountain range. Given its age, the BSRA is an important (and extreme) data point in the New Zealand landslide inventory, and a reminder that older events can be found if we look in the right places.

DATA AVAILABILITY STATEMENT

Datasets are available on request: The data supporting the conclusions of this manuscript will be made available by the author (SM; https://orcid.org/0000-0002-2805-1761), without undue reservation, to any qualified researcher.

AUTHOR CONTRIBUTIONS

SM undertook the planning and collection of all field data (^{10}Be samples, aerial photography, dGPS data collection and post-processing), calculated the ^{10}Be exposure ages (after being provided with atom concentrations from GNS Science and Victoria University of Wellington cosmogenic laboratories), processed the SfM photogrammetry and undertook all geomorphological mapping, and interpretation. Field assistance and field photography was provided by Tom Brookman and Rob McGregor. SM prepared all figures and wrote the manuscript.

FUNDING

Funding was provided by a Massey University research grant RM17927.

ACKNOWLEDGMENTS

I would like to express my gratitude to Rob McGregor and Tom Brookman for their assistance with the fieldwork – for their photographs, help hauling gear and rocks, and their enthusiasm, meat-gathering, and wonderful company. I am grateful to Massey University for funding this research through a MURF grant (RM19927), and to Department of Conservation and staff for permission to carry out this research (Permits 49820-GEO and 49881-FIL). Dr. Jan Blahut is thanked for his proof-reading and helpful discussion. I am also grateful for the constructive feedback provided by reviewers José Darrozes and Fabio Matano.

REFERENCES

Bainbridge, R. (2017). *Lost Landslides: Rock-Avalanche Occurrence and Fluvial Censoring Processes on South Island*. New Zealand PhD Thesis, Northumbria University, Newcastle-upon-Tyne.

Balco, G., Stone, J. O., Lifton, N. A., and Dunai, T. J. (2008). A complete and easily accessible means of calculating surface exposure ages or erosion rates from 10Be and 26Al measurements. *Q. Geochronol.* 3, 174–195. doi: 10.1016/j.quageo.2007.12.001

Ballantyne, C. K., Sandeman, G. F., Stone, J. O., and Wilson, P. (2014). Rock-slope failure following Late Pleistocene deglaciation on tectonically stable mountainous terrain. *Q. Sci. Rev.* 86, 144–157. doi: 10.1016/j.quascirev.2013.12.021

Barrell, D. J. A. (2011). "Quaternary glaciers of New Zealand," in *Developments in Quaternary Science*, Vol. 15, eds J. Ehlers, P. L. Gibbard, and P. D. Hughes (Amsterdam: ScienceDirect), 1047–1064. doi: 10.1016/b978-0-444-53447-7.00075-1

Brocklehurst, S. H., and Whipple, K. X. (2007). Response of glacial landscapes to spatial variations in rock uplift rate. *J. Geophys. Res. F* 112:F02035.

Brook, M. S., Kirkbride, M. P., and Brock, B. W. (2006). Quantified time scale for glacial valley cross-profile evolution in alpine mountains. *Geology* 34, 637–640.

Brook, M. S., Kirkbride, M. P., and Brock, B. W. (2008). Temporal constraints on glacial valley cross-profile evolution: two thumb range, central Southern Alps. New Zealand. *Geomorphology* 97, 24–34. doi: 10.1016/j.geomorph.2007.02.036

Cook, S. J., Porter, P. R., and Bendall, C. A. (2013). Geomorphological consequences of a glacier advance across a paraglacial rock avalanche deposit. *Geomorphology* 189, 109–120. doi: 10.1016/j.geomorph.2013.01.022

Cox, S. C., and Barrell, D. J. A. (2007). Geology of the Aoraki area.**:** institute of Geological and Nuclear Sciences 1:250 000 geological map 215. 271.

Deline, P., Hewitt, K., Reznichenko, N., and Shugar, D. (2015). "Chapter 9 - rock avalanches onto glaciers," in *Landslide Hazards, Risks and Disasters*, eds J. F. Shroder and T. Davies (Boston: Academic Press), 263–319. doi: 10.1016/b978-0-12-396452-6.00009-4

Dufresne, A., and Davies, T. R. (2009). Longitudinal ridges in mass movement deposits. *Geomorphology* 105, 171–181. doi: 10.1016/j.geomorph.2008.09.009

Dunning, S. A., Rosser, N. J., McColl, S. T., and Reznichenko, N. V. (2015). Rapid sequestration of rock avalanche deposits within glaciers. *Nat. Commun.* 6:8964. doi: 10.1038/ncomms8964

Froude, M. J., and Petley, D. (2018). Global fatal landslide occurrence from 2004 to 2016. *Nat. Hazards Earth System Sci.* 18, 2161–2181. doi: 10.5194/nhess-18-2161-2018

Görüm, T. (2019). Tectonic, topographic and rock-type influences on large landslides at the northern margin of the Anatolian Plateau. *Landslides* 16, 333–346. doi: 10.1007/s10346-018-1097-7

Hancox, G. T., Langridge, R. M., Perrin, N. D., Vandergoes, M., and Archibald, G. (2013). *Recent Mapping and Radiocarbon Dating of Three Giant Landslides in Northern Fiordland*. New Zealand: GNS Science, 52.

Hancox, G. T., and Perrin, N. D. (2009). Green Lake Landslide and other giant and very large postglacial landslides in Fiordland, New Zealand. *Q. Sci. Rev.* 28, 1020–1036. doi: 10.1016/j.quascirev.2008.08.017

Hancox, G. T., Perrin, N. D., and Dellow, G. D. (2002). Recent studies of historical earthquake-induced landsliding, ground damage, and MM intensity in New Zealand. *Bull. New Zealand Soc. Earthquake Eng.* 35, 59–95. doi: 10.5459/bnzsee.35.2.59-95

Hatherton, T., and Leopard, A. (1964). The densities of New Zealand rocks. *New Zealand J. Geol. Geophys.* 7, 605–625. doi: 10.1080/00288306.1964.10422108

Hermanns, R. L., Schleier, M., Böhme, M., Blikra, L. H., Gosse, J., vy-Ochs, S. I., et al. (2017). *Rock-Avalanche Activity in W and S Norway Peaks After the Retreat of the Scandinavian Ice Sheet*. Cham: Springer International Publishing.

Hilger, P., Gosse, J. C., and Hermanns, R. L. (2019). How significant is inheritance when dating rockslide boulders with terrestrial cosmogenic nuclide dating?—a case study of an historic event. *Landslides* 16, 729–738. doi: 10.1007/s10346-018-01132-0

Hungr, O. (2006). *Rock Avalanche Occurrence, Process and Modelling*. Dordrecht: Springer Netherlands.

Jiskoot, H. (2011). Long-runout rockslide on glacier at Tsar Mountain, Canadian Rocky Mountains: potential triggers, seismic and glaciological implications. *Earth Surf. Process. Landf.* 36, 203–216. doi: 10.1002/esp.2037

Jones, R. S., Small, D., Cahill, N., Bentley, M. J., and Whitehouse, P. L. (2019). iceTEA: tools for plotting and analysing cosmogenic-nuclide surface-exposure data from former ice margins. *Q. Geochronol.* 51, 72–86. doi: 10.1016/j.quageo.2019.01.001

Kerr, T., Owens, I., and Henderson, R. (2011). The precipitation distribution in the Lake Pukaki catchment. *J. Hydrol. New Zealand* 50, 361–382.

Kirkbride, M. P., and Matthews, D. (1997). The role of fluvial and glacial erosion in landscape evolution: the Ben Ohau Range, New Zealand. *Earth Surf. Process. Landf.* 22, 317–327. doi: 10.1002/(sici)1096-9837(199703)22:3<317::aid-esp760>3.0.co;2-i

Korup, O. (2005). Large landslides and their effect on sediment flux in South Westland, New Zealand. *Earth Surf. Process. Landf.* 30, 305–323. doi: 10.1002/esp.1143

Korup, O. (2008). Rock type leaves topographic signature in landslide-dominated mountain ranges. *Geophys. Res. Lett.* 35:L11402. doi: 10.1029/2008GL034157

Korup, O., and Clague, J. J. (2009). Natural hazards, extreme events, and mountain topography. *Q. Sci. Rev.* 28, 977–990. doi: 10.1016/j.quascirev.2009.02.021

Korup, O., Clague, J. J., Hermanns, R. L., Hewitt, K., Strom, A. L., and Weidinger, J. T. (2007). Giant landslides, topography, and erosion. *Earth Planet. Sci. Lett.* 261, 578–589. doi: 10.1016/j.epsl.2007.07.025

Lee, J., Davies, T., and Bell, D. (2009). Successive Holocene rock avalanches at Lake Coleridge, Canterbury, New Zealand. *Landslides* 6, 287–297. doi: 10.1007/s10346-009-0163-6

McColl, S. T. (2012). Paraglacial rock-slope stability. *Geomorphology* 15, 1–16. doi: 10.1016/j.geomorph.2012.02.015

McColl, S. T., Cook, S. J., Stahl, T., and Davies, T. R. H. (2019). Origin and age of The Hillocks and implications for post-glacial landscape development in the upper Lake Wakatipu catchment, New Zealand. *J. Q. Sci.* 34, 685–696. doi: 10.1002/jqs.3168

McColl, S. T., Davies, T. R. H., and McSaveney, M. J. (2012). The effect of glaciation on the intensity of seismic ground motion. *Earth Surf. Process. Landf.* 37, 1290–1301. doi: 10.1002/esp.3251

McSaveney, M. J., Davies, T. R., and Hodgson, K. A. (2000). "A contrast in deposit style and process between large and small rock avalanches," in *VIII ISL Cardiff, Landslides in Research, Theory and Practice*, (London: Thomas Telford).

Pánek, T. (2014). Recent progress in landslide dating: a global overview. *Progr. Phys. Geogr.* 39, 168–198. doi: 10.1177/0309133314550671

Pánek, T. (2019). Landslides and Quaternary climate changes—The state of the art. *Earth Sci. Rev.* 196:102871. doi: 10.1016/j.earscirev.2019.05.015

Putnam, A. E., Schaefer, J. M., Barrell, D. J. A., Vandergoes, M., Denton, G. H., Kaplan, M. R., et al. (2010). In situ cosmogenic 10Be production-rate calibration from the Southern Alps, New Zealand. *Q. Geochronol.* 5, 392–409. doi: 10.1016/j.quageo.2009.12.001

Reznichenko, N. V., Davies, T. R. H., and Winkler, S. (2015). Revised palaeoclimatic significance of Mueller Glacier moraines, Southern Alps, New Zealand. *Earth Surf. Process. Landf.* 41, 196–207. doi: 10.1002/esp.3848

Rother, H., Fink, D., Shulmeister, J., Mifsud, C., Evans, M., and Pugh, J. (2014). The early rise and late demise of New Zealand's last glacial maximum. *Proc. Natl. Acad. Sci. U.S.A.* 111:11630. doi: 10.1073/pnas.1401547111

Sattler, K. (2016). *Periglacial Preconditioning of Debris Flows in the Southern Alps*. New Zealand: Springer.

Sattler, K., Anderson, B., Mackintosh, A., Norton, K., and de Róiste, M. (2016). Estimating permafrost distribution in the maritime southern Alps, New Zealand, based on climatic conditions at rock glacier sites. *Front. Earth Sci.* 4:4. doi: 10.3389/feart.2016.00004

Schleier, M., Hermanns, R. L., Gosse, J. C., Oppikofer, T., Rohn, J., and Tønnesen, J. F. (2017). Subaqueous rock-avalanche deposits exposed by post-glacial isostatic rebound Innfjorddalen, Western Norway. *Geomorphology* 289, 117–133. doi: 10.1016/j.geomorph.2016.08.024

Shulmeister, J., Davies, T. R., Evans, D. J. A., Hyatt, O. M., and Tovar, D. S. (2009). Catastrophic landslides, glacier behaviour and moraine formation - A view from an active plate margin. *Q. Sci. Rev.* 28, 1085–1096. doi: 10.1016/j.quascirev.2008.11.015

Shulmeister, J., Thackray, G. D., Rittenour, T. M., Fink, D., and Patton, N. R. (2019). The timing and nature of the last glacial cycle in New Zealand. *Q. Sci. Rev.* 206, 1–20. doi: 10.1016/j.quascirev.2018.12.020

Shulmeister, J., Thackray, G. D., Rittenour, T. M., and Hyatt, O. M. (2018). Multiple glacial advances in the Rangitata Valley, South Island, New Zealand, imply roles for Southern Hemisphere westerlies and summer insolation in MIS 3 glacial advances. *Q. Res.* 89, 375–393. doi: 10.1017/qua.2017.108

Stahl, T., Quigley, M. C., and Bebbington, M. S. (2016a). Tectonic geomorphology of the Fox Peak and Forest Creek Faults, South Canterbury, New Zealand: slip rates, segmentation and earthquake magnitudes. *New Zealand J. Geol. Geophys.* 59, 568–591. doi: 10.1080/00288306.2016.1212908

Stahl, T., Quigley, M. C., McGill, A., and Bebbington, M. S. (2016b). Modeling earthquake moment magnitudes on imbricate reverse faults from paleoseismic data: fox peak and forest creek faults, South Island, New Zealand. *Bull. Seismol. Soc. Am.* 106, 2345–2363. doi: 10.1785/0120150215

Stirling, M., McVerry, G., Gerstenberger, M., Litchfield, N., Van Dissen, R., Berryman, K., et al. (2012). National seismic hazard model for New Zealand: 2010 update. *Bull. Seismol. Soc. Am.* 102, 1514–1542.

Strom, A. L. (2010). "Evidence of momentum transfer during large scale rockslides' motion. Geologically active," in *Proceedings of the Delegate Papers 11th Congress of the International Association for Engineering Geology and the Environment, Auckland, Aotearoa, 5-10 September 2010*, eds A. L. Williams, G. M. Pinches, C. Y. Chin, T. J. McMorran, and C. I. Massey (Auckland: CRC Press), 73–86.

Sweeney, C. G., Brideau, M. A., Augustinus, P. C., and Fink, D. (2013). "Lochnagar landslide-dam – Central Otago, New Zealand: geomechanics and timing of the event," in *Proceedings of the 19th NZGS Geotechnical Symposium*, Queenstown, 20–23.

Tatard, L., Grasso, J. R., Helmstetter, A., and Garambois, S. (2010). Characterization and comparison of landslide triggering in different tectonic and climatic settings. *J. Geophys. Res.* 115:F4.

Whitehouse, I. E., and Griffiths, G. A. (1983). Frequency and hazard of large rock avalanches in the central Southern Alps, New Zealand. *Geology* 11, 331–334.

Conflict of Interest: The author declares that the research was conducted in the absence of any commercial or financial relationships that could be construed as a potential conflict of interest.